Low Velocity Impact and Internal Pressure Behaviors of Unaged E-Glass and S-Glass/Epoxy Composite Elbow Pipe Joints

Sujith Bobba[1]; Z. Leman[2]; E. S. Zainudin[3]; and S. M. Sapuan[4]

Abstract: This experimental analysis studies the consequences of impact loading on the impact performance and monotonic burst pressure on the level of leakage after impact of E- and S-glass/epoxy composite pipe joints. First, impact tests with three dissimilar energy points (10, 12.5, and 15 J) were applied on composite elbow pipe joints at room temperature, followed by burst pressure tests. Scanning electron microscopy pictures were taken, and the relationship between levels of impact energy on the pipe joints with burst strength was recognized. The results of proposed S-glass/epoxy composite elbow pipe joints were more prominent when were matched with that of a reference specimen, an E-glass/epoxy composite elbow pipe joint. This research proposes a new perspective that impact strength depends upon the increase in time of impact and type of material used. **DOI: 10.1061/(ASCE)PS.1949-1204.0000493.**

Author keywords: E-glass; S-glass; Composite elbow pipe joints; Impact performance; Level of leakage; Monotonic burst pressure; Impact strength.

Introduction

Glass composite pipe joints are coming to be increasingly utilized for multiple purposes in present times. A pipe joint is prefabricated between two pipe pieces. These pipe joints have an extensive variety of purposes, such as transport of geothermal power and wastewater for submerged purposes, owing to their strength-to-load and rigidity-to-load ratios, heat endurance, and corrosion opposition. In some applications, E-glass composite pipes are subjected to various ecological conditions that can reduce their mechanical properties. They are also sensitive to impact loading and pressure fluctuations, especially the pipe joints. Hence, matrix disintegration and wear-away happens with low-velocity impacts. Matrix cracking and delamination has a very unpredictable effect on the performance of the E-glass material. For instance, the Hebei Spirit oil spill on December 7, 2007, was the nastiest oil spill noted in Korea, with the release of approximately 10,900 t of crude oil due to the high pressure level in the pipelines, leading to around 376 km of seashore being polluted near the west coast of Korea.

[1]Assistant Professor, Faculty of Engineering, Dept. of Mechanical and Manufacturing Engineering, Universiti Putra Malaysia, Serdang 43400, Malaysia; Dept. of Applied Engineering, Vignan's Foundation for Science, Technology and Research, Guntur, Andhra Pradesh 522213, India (corresponding author). ORCID: https://orcid.org/0000-0002-1633-1299. Email: sujith.bobba@mail.com

[2]Associate Professor, Faculty of Engineering, Dept. of Mechanical and Manufacturing Engineering, Universiti Putra Malaysia, Serdang 43400, Malaysia. Email: zleman@upm.edu.my

[3]Associate Professor, Faculty of Engineering, Dept. of Mechanical and Manufacturing Engineering, Universiti Putra Malaysia, Serdang 43400, Malaysia. Email: edisyam@upm.edu.my

[4]Professor, Faculty of Engineering, Dept. of Mechanical and Manufacturing Engineering, Universiti Putra Malaysia, Serdang 43400, Malaysia. Email: sapuan@upm.edu.my

Note. This manuscript was submitted on February 20, 2019; approved on May 21, 2020; published online on July 16, 2020. Discussion period open until December 16, 2020; separate discussions must be submitted for individual papers. This paper is part of the ***Journal of Pipeline Systems Engineering and Practice***, © ASCE, ISSN 1949-1190.

During utilization of glass fiber/epoxy composite pipes, there are prospects of impact loading such as crashing, colliding, and rough handling. One more factor is that the amount of failures in straight-line composite pipes is quite lower than the failures that occur in a composite pipe joints because the flow is turbulent at the pipe joint and fluid flow pressure level is higher when compared with a straight-line pipe joint. Analysis of the issue of the strength depletion of the E-glass composite pipe joint after a low-energy impact is valuable for many applications. In this context, the effect of low-velocity impacts on mechanical parameters such as impact reaction and internal pressure strength of two different types of glass (E-glass and S-glass) fiber-reinforced composite pipe joints is presented.

Many studies have sought to determine the impact behavior of composite pipes. Tests were performed to estimate the failure behavior of prestressed glass-fiber-reinforced pipes set to low-velocity impact (Kara et al. 2015). It was also found that the change in diameter with the change in internal pressures for damaged and nondamaged pipes will be equal. Investigational studies on the causes of the impact energy extent and pipe diameter on the impact and compression after impact behaviors of filament-wound-composite tubes were performed (Deniz et al. 2012). Diameters of the tube were 50, 75, 100, and 150 mm, and impact energy intensities of 15, 20, and 25 J were applied on the various tubes of different diameters at room temperature. It was finally concluded that both specimen diameter and impact energy highly affected the impact response and compression postimpact strength of composite tubes.

Repair of damaged fiber-reinforced composite pipes by covering them externally with composite patches was performed by Kara et al. (2014), and they found out that a six-layered patch is appropriate for the retrofitting of impact-damaged tubes. Studies on the effect of impact loading upon fatigue behavior of hybrid composite pipes concluded that damage before impact could not affect the fatigue life of the pipes (Gemi et al. 2017). Experimental study on the ongoing distortion performance of single-direction pultruded composite tubes exposed to an axial impact load was conducted, and consequences of the geometry shape, initiating, strain rate, and the type of resin on energy engagement into the composite

tubes were analyzed (Palanivelu et al. 2010). Zhou and Greaves (2000) evaluated the impact-wound limits for wide E-glass-polyester and S-glass-phenolic laminates and concluded that impact strength was considerably low to the velocity of impact for E-glass-polyester and S-glass-phenolic laminates, respectively, and finally, the consequences on the geometry of the laminates with respect to shear-out resistance was higher in E-glass-polyester laminates than in S-glass-phenolic laminates.

The consequences of environmental situations on the hydrostatic burst pressure and impact performance of glass-fiber-reinforced thermoset pipes were studied by Naik (2005). Impact reaction of the laminated composite cylindrical shells was decided by Krishnamurthy et al. (2003) by means of a traditional Fourier series and finite-element methods. Zhao and Cho (2004) examined the impact-generated damage commencement and circulation in laminated shells for low-velocity impacts. The damage examination was done by means of the Tsai-Wu quadratic failure criterion. In the analysis performed by them, flat and curved laminates were linked for reviewing the damage procedure. Attained results showed that numerical outcomes validated the experimental outcomes.

Kistler and Waas (1998) investigated the reaction of bent laminated composite boards exposed to drop weight testing, consisting of both minor and major distortions mathematically and experimentally. A nonlinear method of calculations was drawn for the impact setback, and impact tests were also accomplished to validate the studies. Impact force and displacement histories were judged with the test statistics and reports of other researchers for small and large deformations of flat and curved panels.

Hawa et al. (2016) investigated on the effects of water ageing and low-velocity impact loading on E-glass fiber/epoxy composite pipe subjected monotonic internal pressure. The researchers found out that after performing burst pressure tests, weepage and eruption depend on the impact energies applied on the samples. Gning et al. (2005) investigated the description, design of destruction commencement, and failure growth in glass-reinforced epoxy composite cylinders exposed to drop weight impact. They also showed a method to estimate the failure caused due to external pressure loading.

Experimental Details

Material and Sample Preparation

Glass epoxy elbow pipe joints were made manufactured by a hand lay-up process as per ASTM D5685 (ASTM 2011) standard, which shows the typical construction of fiber glass (glass-fiber-reinforced thermosetting resin) pressure pipe fittings by hand lay-up equipment. One layer full wrap of each E-glass and S-glass roving as shown in Fig. 1 is used in the preparation of the specimens. An inner radius of 100 mm, outer radius of 101.75 mm, and finally radius of curvature of R = 1.5D were used as the dimensions for the fabrication of elbow joints.

One elbow joint is manufactured using an E-glass mat supplied by Win-Fung Fiberglass (Selangor, Malaysia), and the other one with the proposed S-mat supplied by AGY Holdings (Aiken, South Carolina). Bisphenol vinyl ester epoxy ETERSET (2960P-5) and

Fig. 1. Fabrication process of E-glass and S-glass elbow joint: (a) mold preparation; (b) applying wax; (c) applying S- and E-mats around the mold; (d) applying resin; (e) completion; and (f) measurement.

Table 1. Mechanical properties of the E-glass fiber, S-glass fiber, and the resin

S. No.	Material description	Tensile strength, σ_{TS} (MPa)	Young's modulus, E (GPa)	Density, ρ (g/cm^3)	Poisson's ratio
1	E-glass	2,400	72.4	2.55	2.5
2	S-glass	4,750	86	2.49	2.8
3	Epoxy resin	80	3.1	1.13	3.5–4.5

hardener were selected as the matrix for E-glass elbow joint, and in the case of the S-glass elbow joint, the N-matrix-type resin N,N diglycidyl-4-glycidyloxyaniline ($C_{15}H_{19}NO_4$) supplied by Sigma-Aldrich (St Louis, Missouri) was cross-linked with metaphenylene-diamine ($C_6H_8N_2$) supplied by Zhejiang Amino-Chem (Shanghai, China), which is typically used for marine applications (Gauchel et al. 1975), as shown in Fig. 3. The mechanical properties of the resin used for E-glass elbow joint fabrication are displayed in the Table 1, but for the S-glass elbow joint, some of the mechanical properties' prediction is still in the research phase.

Composite pipe joints were cooled at room temperature until the pipe joints retained their properties. In the case of the fiber volume fraction (Vf) of the elbow pipe joints, it was predicted from the change in the weight between the fiber rolls after and before the hand-layup process. The mass of the epoxy resin used was finalized by removing the mass of the fiber from the total mass of the pipe joint. When the masses of both the fiber and epoxy are well-known, it is easy to find the fiber volume fraction, By investigation/calculation, it was determined as 58% for the E-glass elbow joint and 55% in the case of the S-glass elbow joint. The wall thickness of each of the pipe joints was approximately 1.75 mm. The E-glass and S-glass elbow pipe joints used for tests and their mechanical properties are presented in Fig. 2 and Table 1.

A total of six elbow pipe joints were used for the tests, in which three were fabricated with E-glass and three were fabricated with S-glass fiber. All the mechanical tests were performed according to ASTM standards on the elbow pipe joints (Fig. 3) [ASTM D2444 (ASTM 2010), ASTM D2992 (ASTM 2018a), ASTM D1599 (ASTM 2018b)].

Experimental Procedure

Impact Tests

Usually, impact resistance, alongside impact strength, is the most commonly considered property and is used to calculate the damage of the composite shapes. Impact damage can be determined by two methods, namely impact damage resistance and damage forbearance. In the present design, impact tests are carried out by utilizing a machine corresponding to ASTM D2444 (ASTM 2010). The impact machine can be operated for various functions from high- to low-impact momentum. The impactor has a hemispherical noselike structure with 12.5 mm diameter, which is installed with a 22.3-kN piezoelectric force transducer. The overall falling mass with the crosshead, impactor nose, and force transducer was 5.04 kg. When performing impact tests, a bounding structure is used to control the specimens from various impacts. Experiments were performed with dissimilar impact energies of 10, 12.5, and 15 J in order to examine the damage development in the different elbow pipe joints at room temperature.

For the impact tests, a unique apparatus was designed and developed. The elbow pipe joints were closed with two glass epoxy lids to create a real elbow joint situation as shown in Fig. 4(c); it rested on the hollow and was secured to the underneath plate of the equipment with four nuts and bolts, as shown in Fig. 4(b). A high-speed camera with Hotshot SC software version 512 was used to predict the contact time between the specimen and impactor as shown in Fig. 5. The contact time of the impactor with the specimen is calculated for every impact energy, and the values are listed in Table 2.

The absorbed energy and deflection from the force-time reaction can be computed by means of a Visual IMPACT software version 6 database experimentally by using a data acquisition (DAQ) system where deflection is calculated by the double integration of acceleration and theoretically using Newton's second law as follows:

$$\delta(t) = \delta i + v_i t + \frac{gt^2}{2} - \int_0^t \left[\int_0^{t'} \frac{F(t'')}{m} dt' \right] dt \tag{1}$$

$$E_a(t) = \frac{1}{2} m[v_i^2 - v_f^2(t)] + mg\delta(t) \tag{2}$$

where δ = displacement of the impactor; δi = impact location; $E_a(t)$ = time t for the absorbed energy; F = force during impact; v_i = starting impact velocity; and m = impactor mass. The impact velocity $v_f(t)$ can be gained as follows:

$$v_f(t) = v_i + gt - \int_0^t \frac{F(t')}{m} dt' \tag{3}$$

Every impact experiment was replicated four different times, and mean values were estimated. Maximum contact force, absorbed energy, and maximum deflection are three significant considerations to estimate the impact performance of the composite elbow pipe joints as stated previously. To check the history of the impact

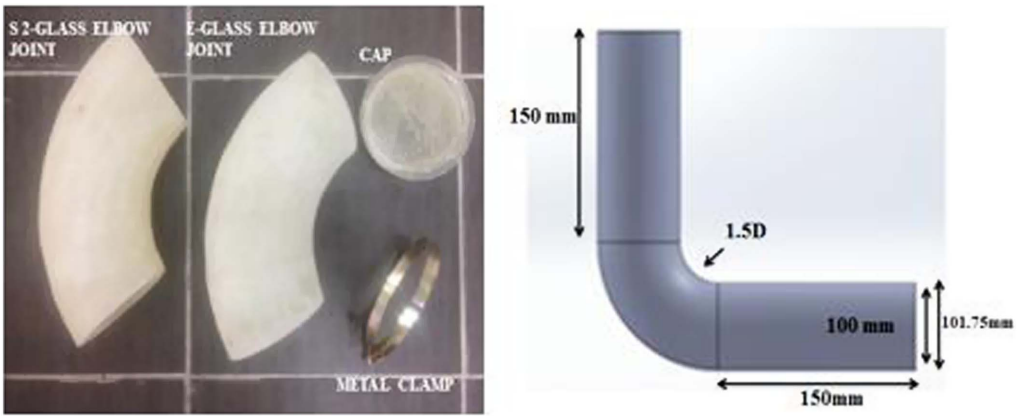

Fig. 2. E-glass and S-glass elbow pipe joints used for tests.

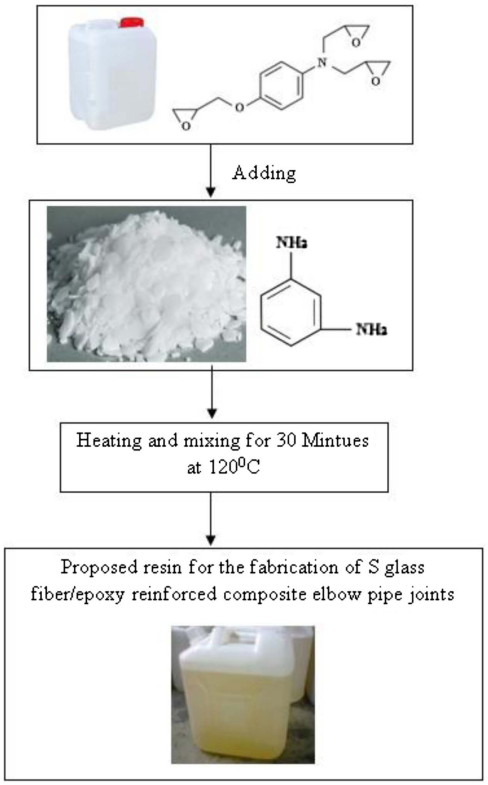

Fig. 3. Preparation of proposed matrix for the fabrication of the S-glass fiber/epoxy reinforced composite elbow pipe joint as per ASTM D5685 (ASTM 2011).

incident, a DAQ was used. The DAQ permits to one acquire an extreme result of 15,000 items of data throughout each test.

Monotonic Burst Tests

In this analysis, internal burst pressure tests were implemented on the elbow pipe joints to decide their practical failure and burst strength after the elbow pipe joints were exposed to different impact energies. The burst tests are executed by using a pressure test rig, which was constructed in according to ASTM D1599 (ASTM 2018b), as shown in Fig. 6. Water was used at room temperature as the pressurizing agent and carefully filled from the inlet. The outlet was closed tightly to prevent water leakage during the test. It was important to drain the complete system around 3–4 min before the test started. This was done to ensure that no air bubbles were trapped in the layers of the elbow pipe joints. The elbow pipe joints were suspended in a relaxed condition by means of rubber rings to guarantee an absolute strain value. It was also ensured that the frame did not restrain the elbow pipe joint along the circumferential or longitudinal directions.

The water-sealed elbow joints are then slowly pressurized up to failure due to the bursting of the elbow pipe joint wall thickness. A pressure transducer was used for the study to calculate the pressure of the water at the impact point; the value are recorded with the help of Labview 17 software to get the accurate leakage and eruption pressures of the pipe joints. A data logger was used along with data acquisition system, and comparison of the results from the data acquisition system with the data logger was carried out. When the pipe curvature is subjected to the internal pressure, the outcomes offer a rise in the stress levels near the cross-section area. The aim of the research is to generate maximum stresses greater than expected and to create effects that have not existed.

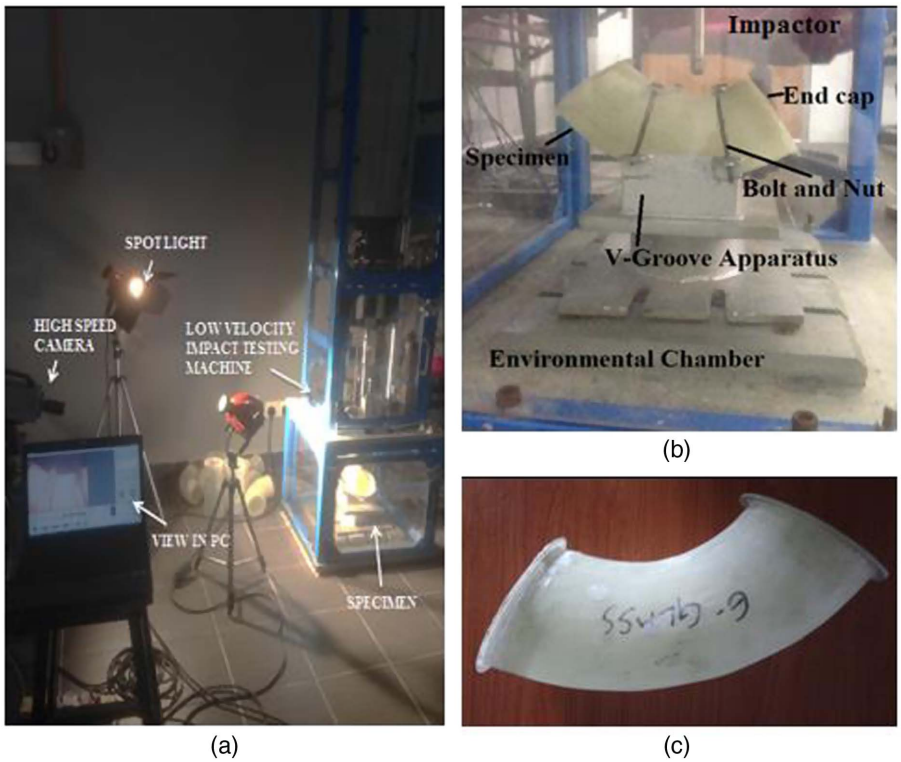

Fig. 4. (a) Setup of IMATEK drop impact testing machine (IMATEK, Knebworth, UK); (b) view of hollow groove test fitting; and (c) sample sealed with two glass fiber/epoxy lids and epoxy glue.

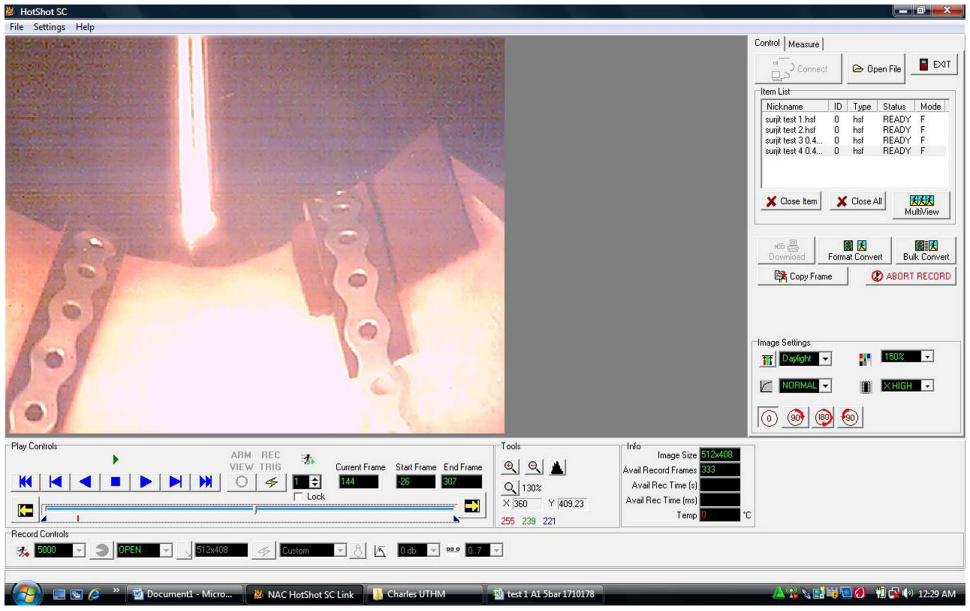

Fig. 5. Hotshot SC software used with a high-speed camera to predict the contact time between specimen and impactor.

Table 2. The values obtained from the force histories (mean values)

Type of elbow joint	Impact energy (J)	Impact velocity (m/s)	Maximum contact force (N)	Contact time (ms)	Maximum displacement (mm)	Impulse force (Ns)	Absorbed energy (J)
E-glass	10	2.16	1,550	9.2	12.27	12.70	8.32
	12.5	3.21	1,560	10.2	12.26	16.58	10.20
	15	4.23	1,540	12.2	11.47	21.94	12.73
S-glass	10	2.14	990	10.2	9.92	12.23	8.80
	12.5	3.20	800	12.3	10.08	15.00	13.20
	15	4.22	700	14.3	9.98	19.23	16.73

Several methods are used to substitute pipe joints that have failed due to clogs or blockages that impede internal flow, but none were successful. When it comes to the point of internal flow in the pipe joints, burst pressure is one of the important factors to calculate the strength of different pipe joints. The burst pressure of a pipe joint can be calculated mathematically by Barlow's formula

$$\text{Burst pressure} = P(D - t)/2t \tag{4}$$

where P = fluid pressure (psi); T = wall thickness of the pipe, which can be the ultimate tensile strength or the yield strength of the material used.

Another factor in the pipe joint failure is due to the hoop stress during internal flow of the fluid in the pipe joint. However, according to the research perspective, only experimental results must be evaluated to calculate the burst pressure of the pipe joints.

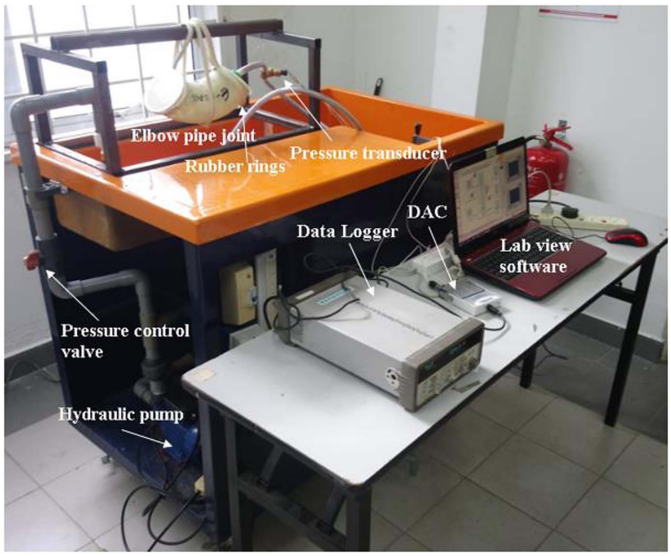

Fig. 6. Monotonic burst pressure test rig designed according to ASTM D1599.

Results and Discussion

Level of Impact Loading

Once the impact energy increased, the highest contact force on the elbow joints was noted, and the importance of impact energy applied is evidently observed to rise in the graphs. Circumferential expansion for the specimens below the influence of different impacts have been noted from Fig. 7, and variations were detected from the graphs that show the damage formed on the elbow joint. The fact that more variations were observed on the graph of the

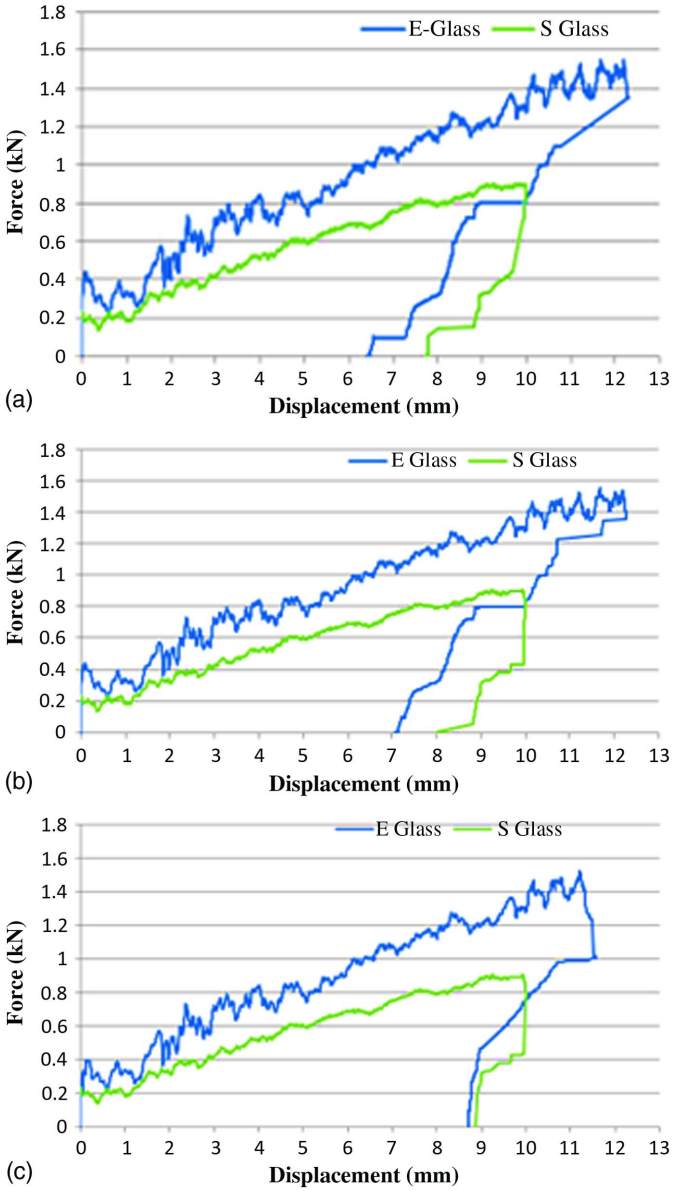

Fig. 7. Force-displacement curves of impacted elbow pipe joints: (a) 10 J; (b) 12.5 J; and (c) 15 J.

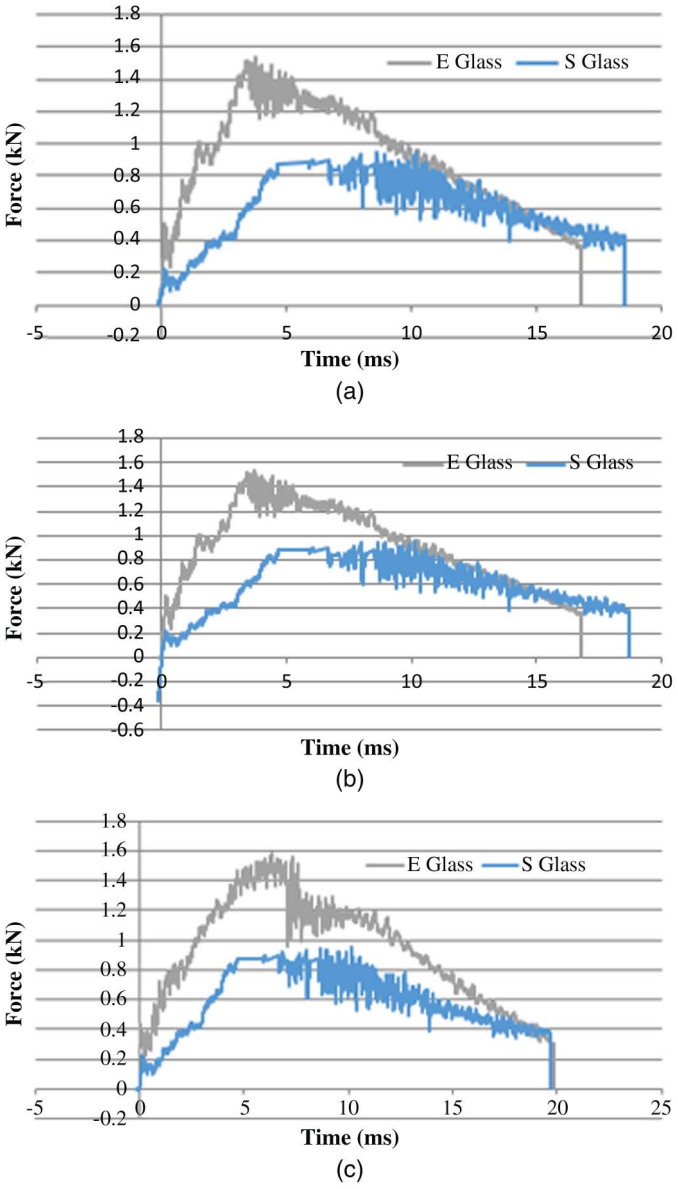

Fig. 8. Contact force time histories of impacted E-glass and S-glass elbow pipe joints: (a) 10 J; (b) 12.5 J; and (c) 15 J.

piece subjected to a 15-J energy level means that a high level of damage has been produced on the sample.

In the force-displacement curves, the E-glass elbow joint showed a considerable increase in level of force in each impact energy, unlike the of S-glass elbow joint, but when it comes in the case of displacement at the final deformation, the S-glass elbow joint showed more interest rather than the E-glass elbow joint. This means that the S-glass elbow joint has a more elastic nature when impacted by a force than the E-glass. In addition, one can predict that the Poisson's ratio of the proposed S-glass elbow joint would be higher compared with that of the E-glass elbow. In some cases, the impact force does not depend on the impact due to displacement, but this depends upon the type of material and matrix used.

The gradient of the force versus displacement curve is the bend-over inflexibility that can be justified, which can be noticed in Fig. 7. There are two distinct features or regimes found from each curve. The first feature can represent the primary indentation. When the contact force commences to curve the pipe joint layer, a minor bending stiffness procedure can be observed. When it reaches to the maximum contact force, the displacement also moves to the maximum position. Beyond that point, the second feature, the rebound regime, clearly starts, and one can notice that throughout impact testing, due to compression stresses in the exterior layers of the pipe joint and tensile stresses in the interior layer of the pipe joints, the matrix breaks appear inside the fiber layer. In addition, the annular surface matrix breaks and delamination occurs in the interior layers.

When it comes to the point of force-time graph in Fig. 8, the same process occurred as occurred in the force-displacement curves, where the E-glass elbow joint showed more impact behavior and less time to withstand the load for breakage. The S-glass elbow joint has taken more time to break by impact than the E-glass. The impact force-time record can show how important the information regarding the damage assessment is, which is why it is proposed to set up a force sensor on the impactor.

One more aspect that can be analyzed from the impact characteristics in the force-displacement and force-time is that maximum

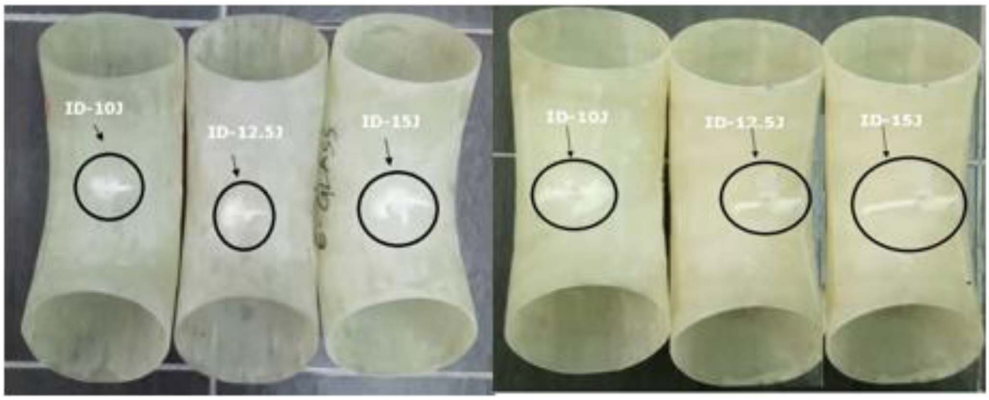

Fig. 9. Damage views of glass/epoxy reinforced elbow pipe joints: (a) E-glass; and (b) S-glass with different impact energies.

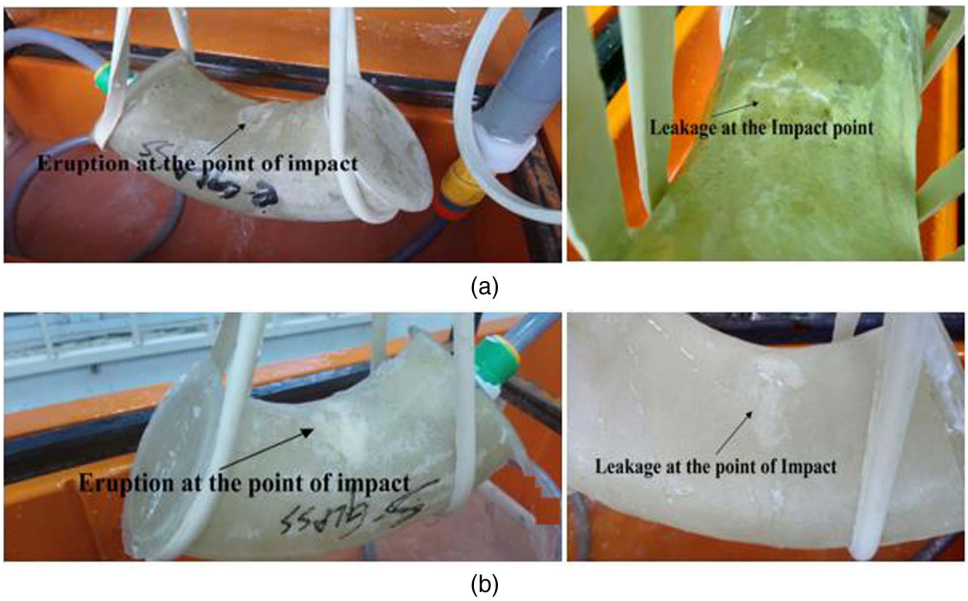

Fig. 10. Leakage damage and eruption damage of nonimpacted elbow pipe joint subjected to internal pressure test: (a) E-glass; and (b) S-glass.

absorbed energy and maximum contact time at final state of various impact energies was by the proposed S-glass elbow joint rather than the E-glass elbow joint. Values obtained from the force histories are given in Table 2.

At intensifying speeds operated by the impactor on the elbow pipe joints, the low-velocity impact has caused damage related to the failure mechanisms in both elbow pipe joints. A lower amount of energy is disbursed at a depleted speed, which caused less damage on the E-glass and S-glass composite elbow pipe joints. Spherical exterior cracks were created on the outer surfaces, particularly for energy levels as high as shown in Fig. 9. In addition, the failure approaches noticed on the composite elbow joints are discovered to be crack commencement, delamination, and fiber/matrix rupture, contingent on the impact energy and type of joint. Finally, absorbed energy can be stated as the momentum spent through the establishment of damage and development of friction. Fig. 10 shows the leakage damage and eruption damage of nonimpacted elbow pipe joints subjected to internal pressure tests.

Burst Strength of the Elbow Pipe Joint

Afterwards, burst pressure tests were performed on the impacted E-glass and proposed S-glass elbow pipe joints at different energy levels under sealed situations. These tests were executed with the purpose of governing the elbow pipe joints' burst-out strength once they were exposed to impact loadings at various energy levels. From Fig. 11, it can be noticed that the burst strength manages to decline with amplifying impact energy. In addition, the elbow pipe joint impacted with an energy extent of 15 J steadily exhibited greater burst pressure than the ones impacted with energy extents of 12.5 and 10 J. Results of burst pressure tests on E-glass and S-glass elbow pipe joints impacted at various energy levels are given in Table 3.

When performing internal burst pressure tests, three different failure approaches were observed: weepage, whitening, and eruption. Weepage failure was witnessed on the elbow pipe joint layer impacted by low energy. As soon the internal pressure escalated more, extra droplets were seen, and later, after considerable

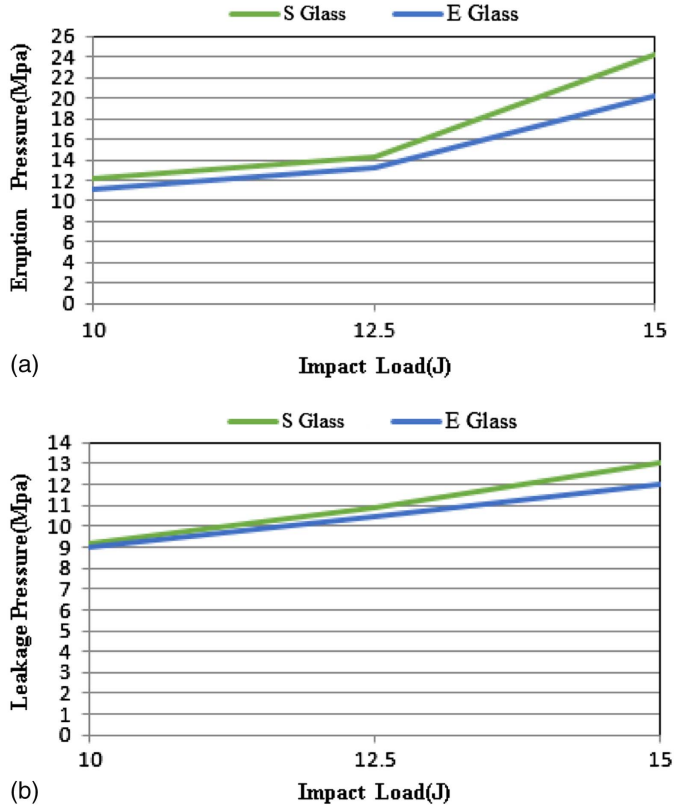

Fig. 11. Comparison between (a) leakage pressure-impact load; and (b) eruption pressure-impact load of E-glass and S-glass elbow pipe joints.

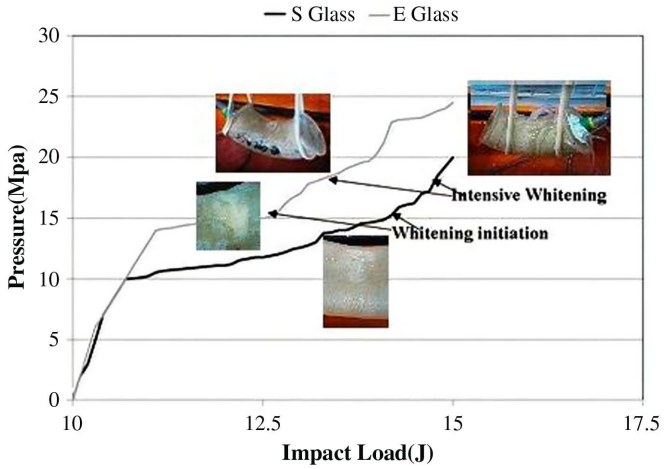

Fig. 12. Internal pressure-impact load for impacted E-glass and S-glass elbow pipe joints.

accumulation, the pipe joint surface was enclosed by water, which subsequently had a leakage from the elbow pipe joint.

Analysis of the examined samples revealed a slight indication of proof of the physical damage with evident white patterns on the external surface of the elbow pipe joint fiber's path, indicating a crack of the matrix inside the laminate structure. Constantly by progress, the eruption failure commenced slowly in the 12.5- and 15-J impact elbow pipe joints. Eruption is a breakdown that happens in an unpredictable method, with considerable fiber rupture around the impact damaged zone. A perceptible breaking sound was overheard just prior to the eruption, which may be connected to the crack development at some point in the tests. The results openly imply that the impact loading has a critical effect on the burst failure pressure of the composite elbow pipe joints. Therefore, an impact's occurrence in a pressured composite elbow pipe joints must be judged in the duration of their existence.

From Fig. 12, it can be noticed that the impact energy has a tendency to change the curve of the elbow pipe joints under the influence of the different types of material (E-glass and S-glass) used. The purpose for this could be described as due to the presence of breaks on fiber as an outcome of the low-velocity impact. Influence of the fibers on the inelasticity of the elbow pipe joints is greater than that of the resin. Prior to the final failure, a pressure decline was detected in the case of elbow pipe joints with impact damages. In the case of sample with E-glass, the impact damage was more than that of S-glass specimen used; however, when the pressure reached 17.23 MPa, the damage was discovered to burst out. As for the sample made of S-glass fiber, it achieved whiteness and then after reaching the pressure of 18.1 MPa, protection in form of whitening developed over the damaged region of the sample, which attained its ultimate failure without any explosion, Finally, it indicates that strong protection occurred in S-glass sample and the sample has attained its ultimate failure state without any detonation when compared with the E-glass sample.

Scanning Electron Microscope for Image Examination

Scanning electron microscope (SEM) representations of the internal and external layers of the leakage zone under pressure tests after impact tests of composite elbow pipe joints are shown in Figs. 13 and 14. It can be seen from Figs. 13 and 14 that there are some matrix cracks, which formed on inner surface of the elbow pipe joint because of the impact loading and internal pressure mostly in E-glass composite elbow joints rather than in the S-glass composite elbow pipe joints. There are dissimilarities in the inner surfaces and outer surface cracks of the elbow joints.

Debonding between fiber and matrix interfaces also appear in the internal plane of the elbow pipe joint, which is not as great as that of the external surface of the elbow pipe joint. These results

Table 3. Summary of monotonic burst tests on E-glass and S-glass elbow pipe joints impacted at various energy levels

Type of elbow joint	Impact energy (J)	Maximum burst pressure (MPa)	Axial stress	Hoop stress	Strain (%)	Failure type
E-glass	10	12.27	132.98	360.88	0.37	Weepage-eruption
	12.5	10.08	109.63	296.47	0.30	Weepage-eruption
	15	8.15	88.83	239.70	0.24	Eruption
S-glass	10	13.80	148.72	405.88	0.41	Weepage
	12.5	12.56	135.85	367.64	0.38	Weepage-eruption
	15	10.13	109.67	297.94	0.30	Weepage-eruption

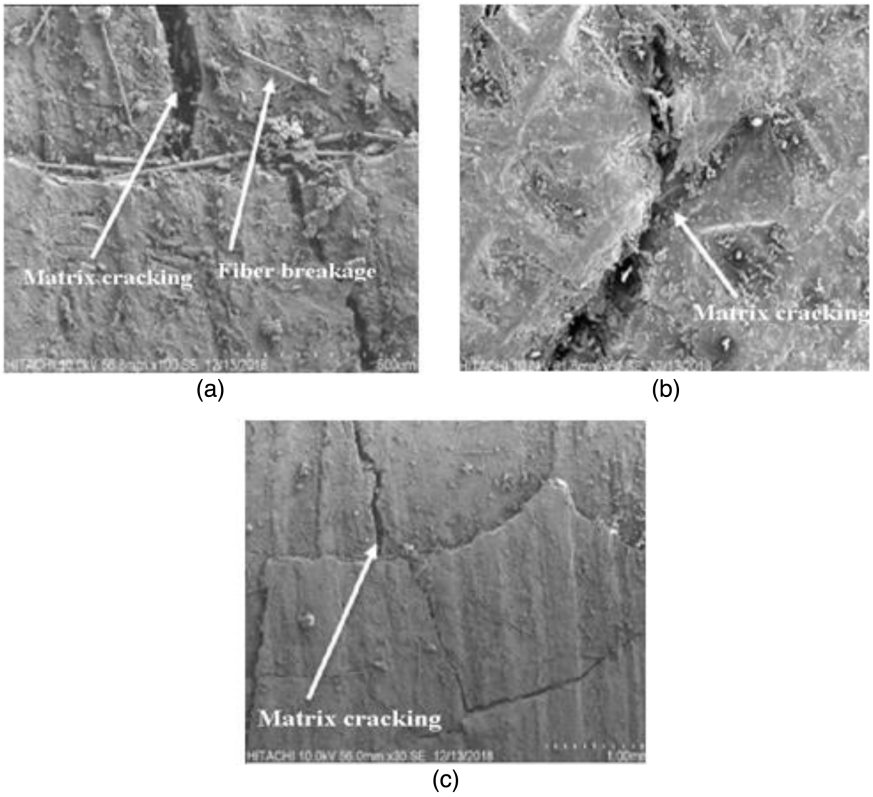

Fig. 13. Micrograph of specimen at leakage and eruption zone after burst pressure tests of E-glass/epoxy composite elbow pipe joints: (a) 10 J; (b) 12.5 J; and (c) 15 J.

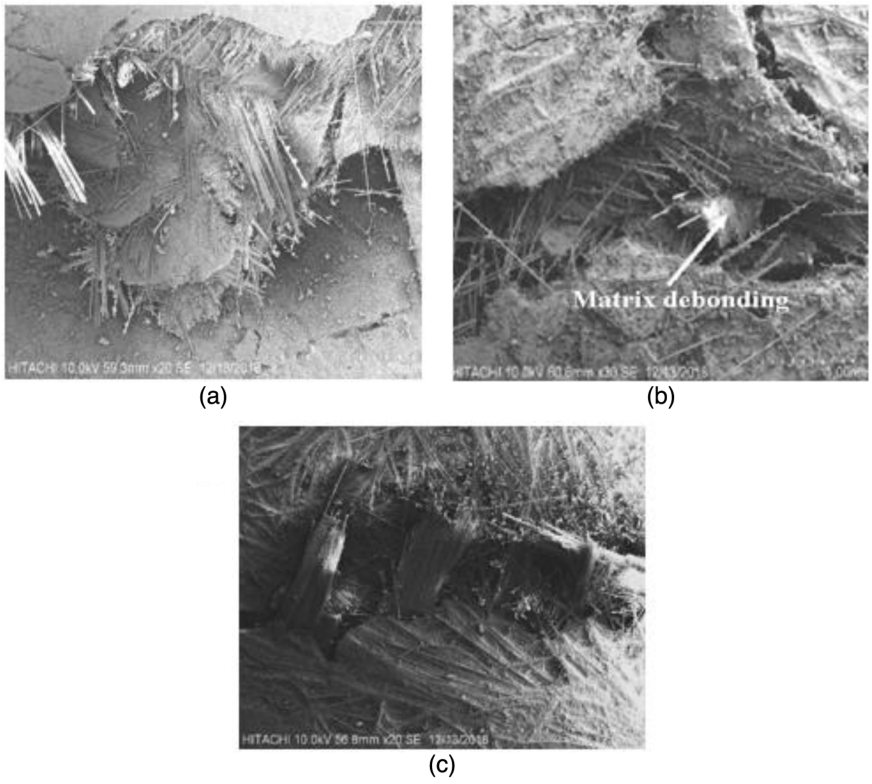

Fig. 14. Micrograph of the samples at leakage and eruption zone after burst pressure tests of S-glass/epoxy composite elbow pipe joints: (a) 10 J; (b) 12.5 J; and (c) 15 J.

are also verified by SEM representations. Eruption and leakage repair of impacted composite joints are generally detected at the end regions and around the impact zone of the specimens.

Conclusion

The subsequent conclusions were obtained based on the results of the impact and internal pressure tests performed on different elbow pipe joints:

- The impact tests graphs clearly show that the displacement notches up to a peak point and then drops from the point of failure primarily in the elbow joints fabricated with E-glass when compared with S-glass elbow pipe joints.
- The impact tests also indicated that the elbow pipe joints made with S-glass fiber, being more flexible, absorb more energy elastically in the final stage of the impact analysis and are not as damaged as the pipe joints made of E-glass fiber for a given impact energy. Accordingly, the proposed S-glass elbow joints have higher Poisson's ratio and yield strength.
- The energy absorbed, maximum displacement, and area of the damage on the pipe joints started to rise as the impact energy rises.
- The higher the impact energy, the higher the connection time interval between the elbow pipe joint and the mass. Also, two diverse features are noticed on the force and displacement graphs, which show the primary depression and bending of elbow pipe joint barrier which already had low rigidity.
- Three different forms of failure were noticed on the elbow pipe joints on the basis of the rise in the inner pressure, commencing with whitening stains in the initial internal pressure examination, which then led to start eruption and weepage damages in both the E-glass and S-glass elbow pipe joints. However, the failure started first in the elbow pipe joint made of the E-glass mat rather than the elbow pipe joint made of the S-glass mat because one factor is due to the impact effects on the E-glass elbow pipe joint and other factor is the internal stability of the pipe joint.

By the preceding conclusions, the authors can justify that the pipe joints (elbow) made of the S-glass mat and the proposed matrix have higher toughness to control the maximum internal pressure and withstand higher impact energies when compared with E-glass mats and epoxy resin used in the construction of onboard and off-board pipelines.

Acknowledgments

The author would like to thank the Universiti Putra Malaysia for supporting this project under Grant by UPM Scheme, Vot No. 9556200.

References

ASTM. 2010. *Standard test method for determination of the impact resistance of thermoplastic pipe and fittings by means of a tup (falling weight)*. ASTM D2444. West Conshohocken, PA: ASTM.

ASTM. 2011. *Standard specification for fiberglass (glass-fiber-reinforced thermosetting-resin) pressure pipe fittings*. ASTM D5685. West Conshohocken, PA: ASTM.

ASTM. 2018a. *Standard practice for obtaining hydrostatic or pressure design basis for "fiberglass" (glass-fiber-reinforced thermosetting-resin) pipe and fittings*. ASTM D2992. West Conshohocken, PA: ASTM.

ASTM. 2018b. *Standard test method for resistance to short-time hydraulic pressure of plastic pipe, tubing, and fittings*. ASTM D1599. West Conshohocken, PA: ASTM.

Deniz, M. E., R. Karakuzu, and M. Sari. 2012. "On the residual compressive strength of the glass–epoxy tubes subjected to transverse impact loading." *J. Compos. Mater.* 46 (6): 737–745. https://doi.org/10.1177/0021998311410483.

Gauchel, J. V., I. Steg, and J. E. Cowling. 1975. "Reducing the effect of water on the fatigue properties of S-glass epoxy composites." In *Fatigue of composite materials*, edited by J. R. Hancock, 45–52. West Conshohocken, PA: ASTM.

Gemi, L., Ö. S. Şahin, and A. Akdemir. 2017. "Experimental investigation of fatigue damage formation of hybrid pipes subjected to impact loading under internal pre-stress." *Composites, Part B* 119 (Jun): 196–205. https://doi.org/10.1016/j.compositesb.2017.03.051.

Gning, P. B., M. Tarfaoui, F. Collombet, and P. Davies. 2005. "Prediction of damage in composite cylinders after impact." *J. Compos. Mater.* 39 (10): 917–928. https://doi.org/10.1177/0021998305048733.

Hawa, A., M. A. Majid, M. Afendi, H. F. A. Marzuki, N. A. M. Amin, F. Mat, and A. G. Gibson. 2016. "Burst strength and impact behaviour of hydrothermally aged glass fibre/epoxy composite pipes." *Mater. Des.* 89 (Jan): 455–464. https://doi.org/10.1016/j.matdes.2015.09.082.

Kara, M., M. Uyaner, and A. Avci. 2015. "Repairing impact damaged fiber reinforced composite pipes by external wrapping with composite patches." *Compos. Struct.* 123 (May): 1–8. https://doi.org/10.1016/j.compstruct.2014.12.017.

Kara, M., M. Uyaner, A. Avci, and A. Akdemir. 2014. "Effect of non-penetrating impact damages of pre-stressed GRP tubes at low velocities on the burst strength." *Composites, Part B* 60 (Apr): 507–514. https://doi.org/10.1016/j.compositesb.2014.01.003.

Kistler, L. S., and A. M. Waas. 1998. "Experiment and analysis on the response of curved laminated composite panels subjected to low velocity impact." *Int. J. Impact Eng.* 21 (9): 711–736. https://doi.org/10.1016/S0734-743X(98)00026-8.

Krishnamurthy, K. S., P. Mahajan, and R. K. Mittal. 2003. "Impact response and damage in laminated composite cylindrical shells." *Compos. Struct.* 59 (1): 15–36. https://doi.org/10.1016/S0263-8223(02)00238-6.

Naik, M. K. 2005. *The effect of environmental conditions on the hydrostatic burst pressure and impact performance of glass fiber reinforced thermoset pipes*. Dhahran, Saudi Arabia: King Fahd Univ. of Petroleum and Minerals.

Palanivelu, S., W. Van Paepegem, J. Degrieck, J. Van Ackeren, D. Kakogiannis, D. Van Hemelrijck, J. Wastiels, and J. Vantomme. 2010. "Experimental study on the axial crushing behaviour of pultruded composite tubes." *Polym. Test.* 29 (2): 224–234. https://doi.org/10.1016/j.polymertesting.2009.11.005.

Zhao, G., and C. Cho. 2004. "On impact damage of composite shells by a low-velocity projectile." *J. Compos. Mater.* 38 (14): 1231–1254. https://doi.org/10.1177/0021998304042084.

Zhou, G., and L. J. Greaves. 2000. "Damage resistance and tolerance of thick laminated woven roving GFRP plates subjected to low-velocity impact." In *Impact behaviour of fibre-reinforced composite materials and structures*, 133–185. Cambridge, UK: Woodhead.